RESEARCH ARTICLE
Cytoskeleton, May 2015 72:235–245 (doi: 10.1002/cm.21223)

Structured Illumination Microscopy Reveals Focal Adhesions are Composed of Linear Subunits

Shiqiong Hu,[1] Yee-Han Tee,[1] Alexandre Kabla,[1,2] Ronen Zaidel-Bar,[1] Alexander Bershadsky,[1,3] and Pascal Hersen[1,4]*

[1]*The Mechanobiology Institute, National University of Singapore, 5A Engineering Drive 1, Singapore 117411, Singapore*
[2]*Engineering Department, Cambridge University, Trumpington Street, Cambridge CB2 1PZ, UK*
[3]*Department of Molecular Cell Biology, Weizmann Institute of Science, Rehovot 76100, Israel*
[4]*Laboratoire Matière et Systèmes Complexes, UMR 7057 CNRS and Université Paris Diderot, 10 Rue Alice Domon et Léonie Duquet, Paris 75013, France*

Received 11 November 2014; Revised 14 April 2015; Accepted 8 May 2015
Monitoring Editor: Pekka Lappalainen

The ability to mechanically interact with the extracellular matrix is a fundamental feature of adherent eukaryotic cells. Cell–matrix adhesion in many cell types is mediated by protein complexes called focal adhesions (FAs). Recent progress in super resolution microscopy revealed FAs possess an internal organization, yet such methods do not enable observation of the formation and dynamics of their internal structure in living cells. Here, we combine structured illumination microscopy (SIM) with total internal reflection fluorescence microscopy (TIRF) to show that the proteins inside FA patches are distributed along elongated subunits, typically 300 ± 100 nm wide, separated by 400 ± 100 nm, and individually connected to actin cables. We further show that the formation and dynamics of these linear subunits are intimately linked to radial actin fiber formation and actomyosin contractility. We found FA growth to be the result of nucleation of new linear subunits and their coordinated elongation. Taken together, this study reveals that the basic units of mature focal adhesion are 300-nm-wide elongated, dynamic structures. We anticipate this ultrastructure to be relevant to investigation of the function of FAs and their behavior in response to mechanical stress. © 2015 Wiley Periodicals, Inc.

Key Words: focal adhesion; structured illumination microscopy; paxillin; mechanobiology; cytoskeleton; cell mechanics

Additional Supporting Information may be found in the online version of this article.

*Address correspondence to: Pascal Hersen; Université Paris Diderot and CNRS, Physics, Paris, France. E-mail: pascal.hersen@univ-paris-diderot.fr

Published online 25 May 2015 in Wiley Online Library (wileyonlinelibrary.com).

Introduction

Cells are mechanically active. Their internal machinery employs elaborate signaling pathways and adhesion proteins to apply forces on their substrate and neighboring cells and to 'feel' their mechanical environment [Geiger et al., 2009; Vogel, 2006; Vogel and Sheetz, 2006]. The ability to adhere to the extracellular matrix (ECM) is a fundamental feature of adherent higher eukaryotic cells and is essential for a variety of key cellular processes, including cell migration, proliferation and differentiation [Discher et al., 2005; Seong et al., 2013; Winograd-Katz et al., 2014]. Thus, it is no surprise that the study of how cells sense the mechanical and geometrical cues in their microenvironment is an active and rapidly expanding field of research, currently termed *mechanobiology* [Eyckmans et al., 2011]; such research is concerned with a wide range of aspects from protein structures to tissue-scale mechanics [Guo et al., 2013].

Focal adhesions (FAs) are one of the primary structures by which cells adhere to the ECM. The transmembrane adhesion receptors in FA are integrins, of which different isoforms bind different ECM proteins (e.g., fibronectin, vitronectin, and collagen) via their extracellular domains. At the same time, integrins bind via their cytoplasmic tails to a complex network of proteins, termed the adhesion plaque. The adhesion plaque is composed of a variety of proteins including talin, vinculin, paxillin, zyxin, and focal adhesion kinase (FAK), to name but a few [Zaidel-Bar et al., 2007]. These plaque proteins exert structural and regulatory roles; chiefly, linking integrins to the actin cytoskeleton. Although the importance of actomyosin contractility in the development of FAs is well-established [Vicente-Manzanares et al., 2009], understanding the molecular nature of the connections between actin and FAs requires novel techniques to characterize adhesion plaque dynamics.

High-resolution microscopy methods have been used to observe the spatial features of FAs at a submicronic scale. Patla *et al*. used cryo-electron tomography and observed three-dimensional doughnut-shaped particles of ~25 nm inside the core of FAs as well as numerous actin filaments [Patla, 2010]. Franz and Muller [2005] used atomic force microscopy to also demonstrate the existence of actin filaments inside FAs. More recently, progress in super resolution microscopy enabled determination of the relative positioning of the proteins within FAs. Kanchanawong et al. [2010] used interferometric photoactivated localization microscopy (iPALM) to visualize the vertical organization of FA proteins in fixed U2OS (human bone osteosarcoma) and MEF (mouse embryonic fibroblast) cells. The structure of FAs in the plane of the substrate has also been observed using photoactivated localization microscopy (PALM) [Shroff et al., 2007]. Such observations have demonstrated that—in fixed cells—FAs are not homogeneous spatial structures, and on the contrary, they contain patches of adhesion proteins with submicron dimensions.

Despite the fact that FAs are highly dynamic structures, the morphological observations described above were obtained using fixed cells. FAs formation is usually observed at the lamellipodium–lamellum interface where they grow along the direction of local actin retrograde flow [Alexandrova et al., 2008; Gardel et al., 2008]. Formation of FAs is initiated by integrin–matrix binding at the leading edge of a cell [nascent adhesions; Vicente-Manzanares et al., 2007]. Nascent adhesions are usually observed as small foci of fluorescence whereas mature FAs have polar and elongated morphologies, extending to several micrometers long and a few micrometers wide. Elongation of FAs has been investigated in detail using TIRF microscopy. In particular, Guo et al. [2007] studied retrograde flux of zyxin and VASP, and Hu et al. [2007] used fluorescent speckle TIRF microscopy (FSM–TIRF) to determine the spatial relationships between retrograde flow of F-actin and several FA proteins (vinculin, talin, paxillin, zyxin, and FAK).

It is now commonly accepted that FAs have a complex internal organization and are dynamic structures. In contrast to super resolution microscopy methods, the resolution offered by the classic TIRF method, which has been used to assess the dynamics of FAs, does not enable the observation of any well-defined internal structure: adhesions simply appear as large, homogeneous plaques displaying internal retrograde flow of proteins. Thus, the dynamics of the internal structure of FAs observed using high resolution microscopy is still a mostly unexplored territory.

Thus, the objective of this study was to observe FAs at a high spatial resolution in live cells. To do so, we combined structured illumination microscopy (SIM) with total internal reflection fluorescence microscopy (TIRFM) to observe REF52 fibroblast cells. The theoretical resolution of SIM is twice that of conventional TIRF [Gustafsson, 2000] (i.e., typically, 100 nm structures can be resolved using SIM) while allowing live imaging (under standard conditions, the acquisition rate is typically a few high-resolution images per minute). Therefore SIM provides an excellent tradeoff between conventional microscopy (low spatial resolution, high frame rate) and super resolution methods (fixed cells at a high spatial resolution). Another implicit limitation imposed by the quantitative study of FAs comes from the large variations in their shape and dynamics, which depend on the cell state and, in particular, its polarity and migratory status [Prager-Khoutorsky, et al., 2011; Smilenov, 1999]. To obtain reproducible FAs, we studied cells seeded on fibronectin-coated disks. Cells cultured on such substrates display the formation of numerous, dynamics FAs close to the edge of the fibronection coated surface.

Using this approach, we show here that FAs are composed of parallel arrays of evenly-spaced linear subunits, each linked at its proximal tip to a single F-actin filament. These linear subunits elongate over time up to a few micrometers long, but maintain a constant width of about 300 ± 100 nm. FAs enlarge when new filaments with approximately the same width are created parallel to the first mother filament, in a well-synchronized dynamic process. Finally, we demonstrate that maturation of these subunits is positively linked to actomyosin contractile activity.

Results

Proteins in FAs are Organized in Periodically Spaced Linear Subunits

In order to investigate the structure and dynamics of FAs at a high spatial resolution, we imaged several FA proteins in REF52 cells. Kanchanawong *et al*. divided FAs into three functional layers (Fig. 1): an integrin signaling layer, a force transduction layer and an actin regulatory layer [Kanchanawong et al., 2010]. Thus, we examined the organization of representative proteins from each of these layers by expressing specific FA proteins fused to fluorescent tags (Fig. 1, see also Supporting Information Movies 1). Integrin $\beta 1$ (Figs. 1A and 1F), FAK (Figs. 1B and 1G) and paxillin (Figs. 1C and 1H) were used to represent the integrin signaling layer; vinculin (Figs. 1D and 1I), the force transduction layer; and zyxin (Figs. 1E and 1J), the actin regulation layer. Images were captured using a SIM–TIRF microscope. To minimize cell variability in these experiments, we imaged cells seeded on homogeneous fibronectin-coated disks of equal diameter (50 μm, see "Methods" and Supporting Information Fig. 3). SIM–TIRF images, for which the resolution typically reached ~100 nm, showed that all of the fluorescent proteins were organized as quasi-periodic linear sets of several (typically 2–10) thin filaments (Fig. 1L). This inner structure was particularly obvious on time lapse images (see Supporting Information Movies SM1). The typical width of these linear subunits was 300 ± 100 nm (Figs. 2B and 2E–2H), regardless of the fluorescent protein

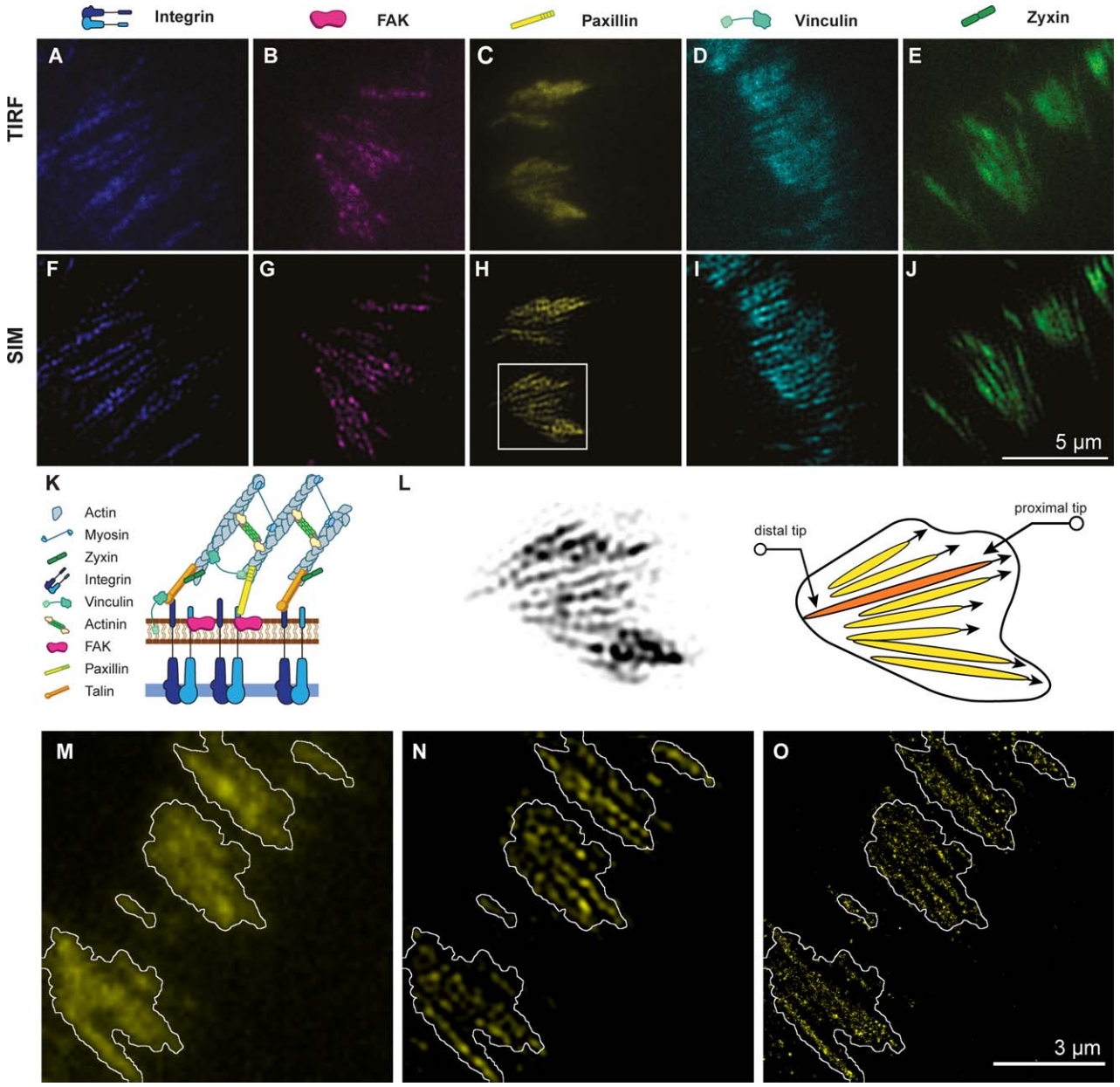

Fig. 1. Focal adhesions are composed of arrays of linear subunits. **A**–**J**: Images of integrin β1-eGFP, FAK–GFP, paxillin–YFP, vinculin–mCherry, and zyxin–GFP obtained using total internal reflection microscopy (TIRF; **A**–**E**) and structured illumination microscopy–total internal reflection microscopy (SIM–TIRF; **F**–**J**). Focal adhesion proteins were observed as large, relatively homogeneous patches using TIRF, whereas SIM–TIRF reveals them to be composed of an array of linear, parallel subunits. **K**: Illustration of the vertical organization of a focal adhesion. **L**: Magnified view of panel H (left) and sketch of the internal structure of this patch (right). The FA plaque (black contour) is composed of an array of linear subunits which extend toward the center of the cell. The proximal tip of the FA subunit is defined as the FA tip closer to cell center, and the distal tip is the FA tip closer to cell edge. **M**–**O**: REF52 cells expressing the photoswitchable protein paxillin–tdEos were fixed and imaged using three different microscopy techniques: TIRF (M), SIM–TIRF (N), and stochastic optical reconstruction microscopy (STORM, O), confirming that SIM–TIRF provides a high fidelity picture of the linear subunits observed using STORM. The white contour indicated the localization of the FA plaque as seen by TIRF (M).

observed. In contrast, the proteins were seen as a continuous fluorescent patch when observed using conventional TIRF microscopy (Figs. 1A–1E). We further studied the colocalization of three of these proteins (paxillin, vinculin, and zyxin) using dual color SIM (Fig. 3): these proteins colocalized with linear FA subunits. This data suggests the linear subunits observed within FAs contain core proteins from all functional layers of the FA, whereas the space between the subunits appears to be devoid of these FA proteins.

To confirm that the linear arrays of filaments observed in FAs using SIM–TIRF were not an artifact of structured illumination, we imaged tdEOS–paxillin-expressing REF52

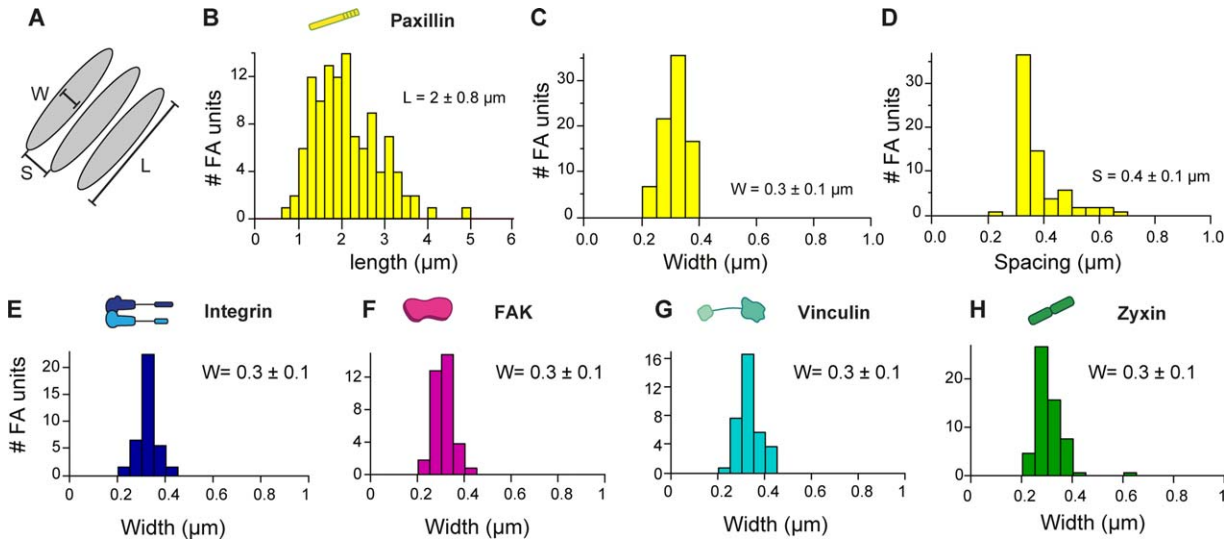

Fig. 2. Focal adhesion subunits have a well-defined width. **A**: Sketch of focal adhesion (FA) linear subunits of width W, length L, and interspacing S. **B–D**: Morphologies of focal adhesion linear subunits in REF-52 cells stably expressing paxillin–YFP. Length was largely distributed between 1 and 5 μm; however, the width and spacing of linear units peaked around 300 ± 100 nm (histograms were based on measurements of 80 linear subunits from 25 focal adhesions in 11 cells). **E–H**: Distribution of the width of the linear subunits measured for the proteins integrin β1-eGFP (E), FAK–GFP (F), vinculin–mCherry (G), and zyxin–GFP (H). The distributions peaked around the same average value of 300 ± 100 nm (four different cells and 40, 35, 36, 58 linear subunits respectively for E–H), demonstrating that the observed morphology does not depend on the type of protein.

cells cultured on fibronectin-coated disks using another high resolution microscopy method, stochastic optical reconstruction microscopy (STORM). As shown in Figures 1M–1O, the same linear filaments observed using SIM–TIRF were also visualized using STORM. Considering the long acquisition period required for STORM imaging, SIM–TIRF appears to be an optimal tool to study both the properties and dynamics of these newly observed FA subunits. Finally, using paxillin as a proxy for FA structure, we confirmed that these subunit arrays were also observed in migratory cells and cells spread on fibronectin-coated patterns with a different geometry (Supporting Information Fig. S1), demonstrating that the presence of arrayed linear FA subunits is a general feature of REF52 cells and is not unique to adherence to circular patterns. We also observed these linear subunits in different cell types (HeLa, HUVEC, and 3T3 MEF cells; Supporting Information Figs. S2A–S2I). However, we did not observe obvious the presence of linear subunits in the small FA of U2OS cells (Supporting Information Figs. S2J–S2L). In the remaining experiments, we used paxillin–YFP as a proxy for FA inner structure.

Linear Subunits Elongate Over Time but Maintain a Constant Width

The advantage of the SIM–TIRF methodology over other super resolution techniques, such as STORM, is its ability to record data in living cells at a temporal resolution of less than a minute. We therefore used SIM–TIRF to elucidate the morphologies (Fig. 2) and dynamics (Fig. 4) of the FA subunits in REF-52 cells stably expressing paxillin–YFP. To get quantitative, reproducible measurements in an automated way, we extracted the width and spacing of linear subunits using 2D autocorrelation of a region of interest containing an array of FA subunits (see "Materials and Methods"). The length was obtained directly from the intensity profile of the images. Interestingly, the width of the linear subunits and the spacing between two linear subunits of the same FA were very well-defined, with a narrow distribution of both width and spacing that peaked around 300 and 400 nm, respectively (±100 nm; Figs. 2C and 2D). In contrast, the length of the linear subunits (around 2 ± 0.8 μm) was more variable (Fig. 2B). However, although the length of the FAs changed over time, their spacing and width remained constant. Tracking the morphological changes of single filaments (Figs. 4A and 4C), we measured their elongation rate to be in the range of 0.1–0.8 μm/min, in agreement with retrograde flow for FA patches observed using TIRF [Alexandrova et al., 2008; Gardel et al., 2008; Guo and Wang, 2007]. More precisely, the elongation rate of single filaments was variable, but around 0.3 μm/min on average (Fig. 4D). Elongation events occurred primarily at the proximal tip of the FA (closer to the center of the cell, Fig. 1L) and in the direction of actin retrograde flow, and were followed by variable periods of rest and sudden shortening or global disappearance (Figs. 4B and 4C). We note that the changes in FA size is not the result of photobleaching, since changes of brightness that occurred by photobleaching appear to be significantly slower. In contrast with elongation dynamics,

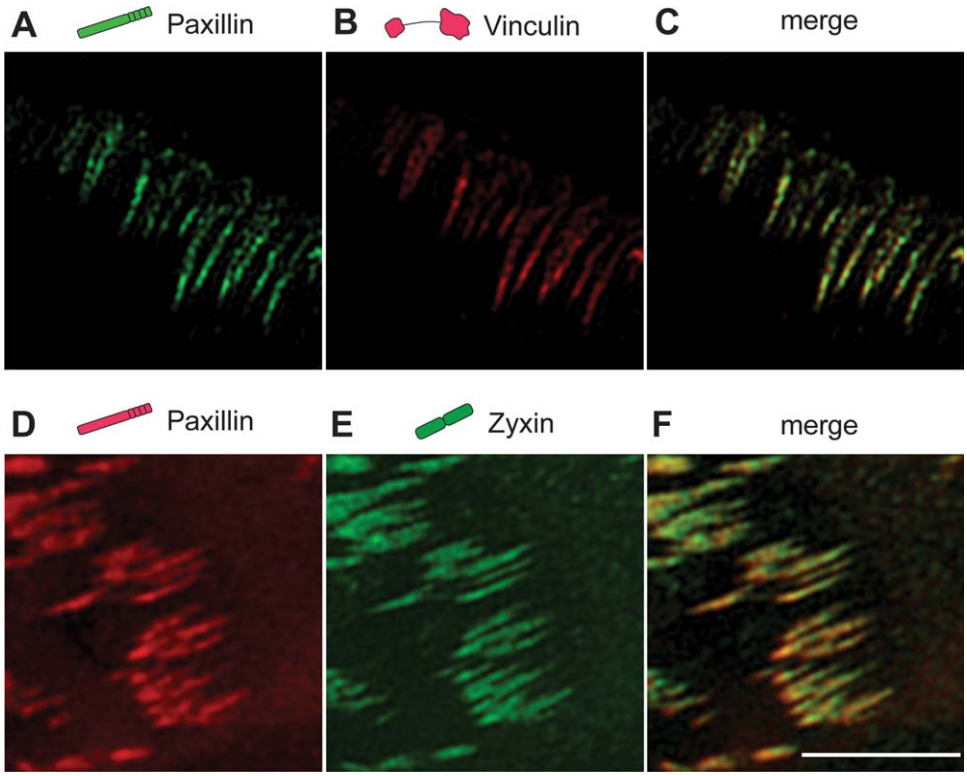

Fig. 3. Linear focal adhesion subunits are composed of several adhesion proteins. **A–C**: REF52 cells doubly transfected with paxillin–eGFP (A) and vinculin–mCherry (B); paxillin and vinculin were shown to colocalize as linear subunits when the images were merged (C). **D–F**: REF52 cells doubly transfected with paxillin–mApple (D) and zyxin–eGFP (E); these focal adhesion proteins also colocalized as linear subunits (F). This demonstrates that paxillin, vinculin and zyxin are components of the same linear subunits. Scale bar is 5 μm. [Color figure can be viewed in the online issue, which is available at wileyonlinelibrary.com.]

shortening primarily occurred at the distal tip—i.e. closer to the lamellipodium (Fig. 4A). FA plaques contained in average six linear subunits (Fig. 4E) and the average lifetime of a single linear subunit was 27 ± 13 min (Fig. 4F). This justifies the importance of using SIM–TIRF to image FAs at both a high enough spatial resolution to distinguish individual subunits and a high enough temporal acquisition rate to observe their dynamics.

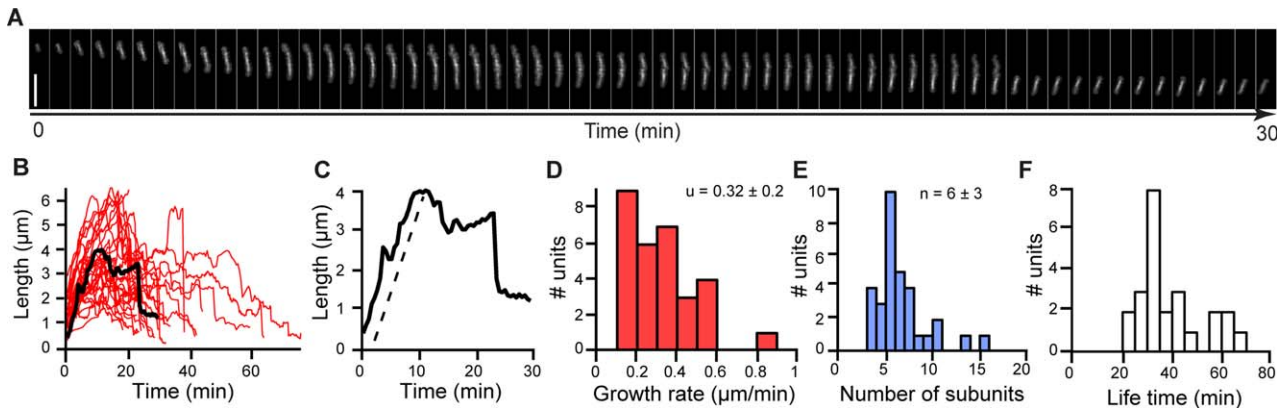

Fig. 4. Focal adhesion linear subunit dynamics. We extracted the dynamic properties of single focal adhesion linear subunits. **A**: Time-lapse images of a typical linear subunit which showed a relatively rapid elongation (around 0.32 μm/min); elongation primarily occurred via extension of the proximal tip (closer to the center of the cell). The vertical scale bar is 3 μm. **B**: Length as a function of time for 30 linear subunits in four different cells. **C**: Evolution of the length of a typical linear subunit (shown in black on panel B) as a function of time. The slope of the first part of the curve (dashed line) is a measurement of the average growth rate. **D–F**: Histograms of the growth rate (u), the number of subunits in a FA plaque and the lifetime of these 30 linear subunits. [Color figure can be viewed in the online issue, which is available at wileyonlinelibrary.com.]

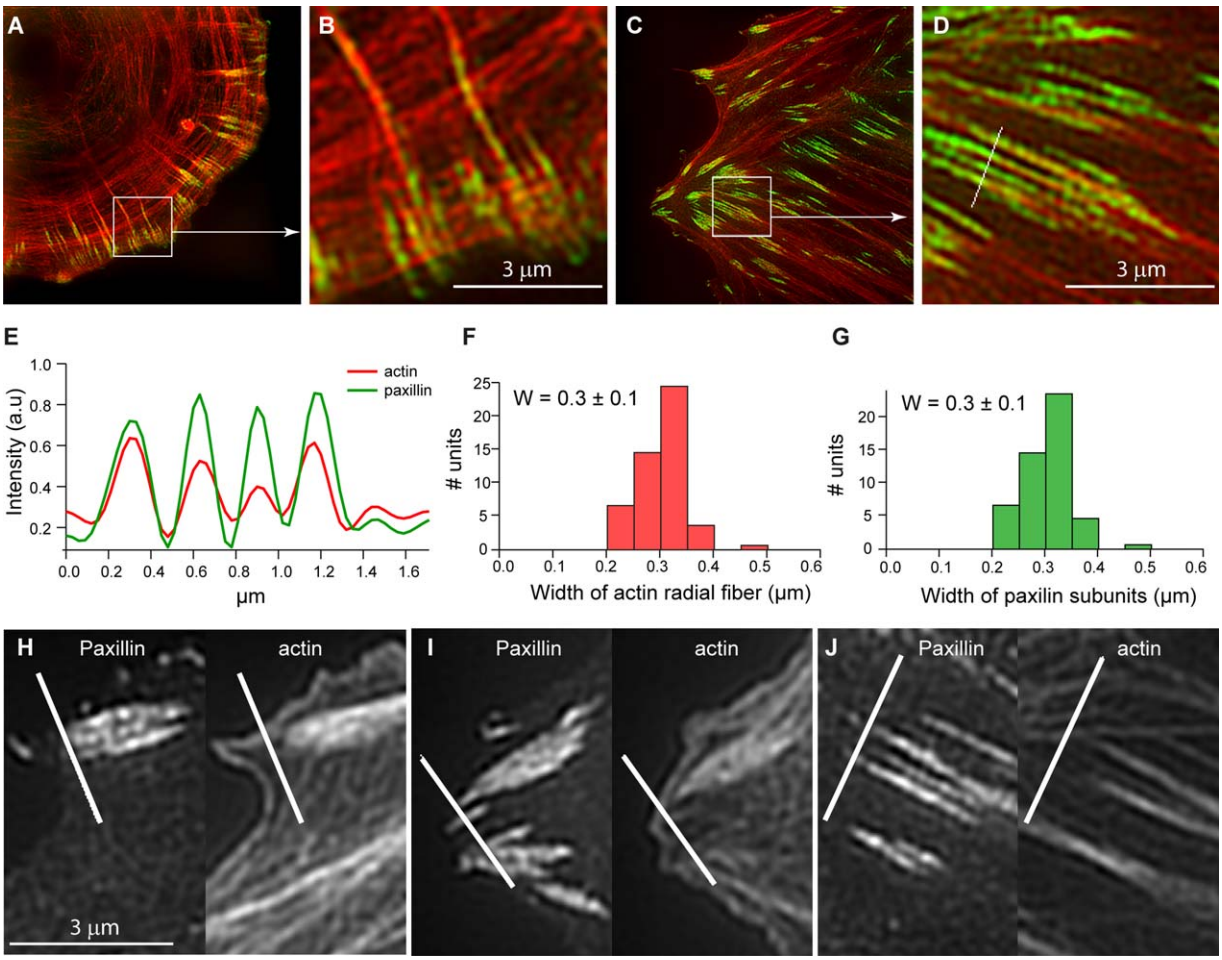

Fig. 5. Focal adhesion linear subunits are linked to individual actin radial fibers at their proximal tip. **A**, **B**: REF52 cells were seeded for 10 h on a circular fibronectin pattern (diameter 50 µm) and labeled with phalloïdin-594 (F-actin) and paxillin–YFP. The images were acquired using dual color SIM. In the magnified panel, one can see how actin radial fibers colocalize with paxillin linear focal subunits. **C, D**: The same analysis for REF52 cells incubated for 3 h on fibronectin-coated glass coverslips. **E**. Monitoring the fluorescence intensity of both actin and paxillin showed that both structures aligned and are in the order of 300 nm wide. **F–G**: Additional measurements (five different cells, 52 linear subunits/actin radial fibers) confirmed that—where they colocalized—the width of both the paxillin filaments and actin radial fibers was similar and that this width was on average around 300 nm. **H–J**: Careful analysis of SIM images of actin (right) and paxillin (left) showed that actin connects to paxillin filaments; however, the actin radial fibers did not extend to the distal tip of the filaments. Straight lines are here as a guide to the eyes. [Color figure can be viewed in the online issue, which is available at wileyonlinelibrary.com.]

Linear FA Units Are Individually Linked to Separate Actin Cables

We then investigated the relationship between FAs and the actin cytoskeleton. To this end, we first used dual color SIM microscopy to image fixed REF52 cells doubly labeled with Phalloidin 594 (F-actin) and paxillin–YFP (Figs. 5A–5D). We found that FA linear subunits were linked to individual actin radial cables (Figs. 5B and 5D). Note that conventional microscopy would not have enabled the resolution of individual actin cables. Actin cables have the same width as adhesion filaments (around 300 nm, Figs. 5E–5G). Interestingly, although actin cables always associated will the proximal tip of FA linear subunits, they did not always extend all the way to the distal tip (Figs. 5H–5J). This result is in agreement with previous results from B. Geiger's lab (Wolfenson et al., 2009). To examine the link between actin and FA linear subunit dynamics, we either decreased or increased actomyosin contractility while simultaneously following the dynamics of linear subunits (Fig. 6). As expected, rapid shortening of all FA linear subunits was observed when actomyosin contractility was decreased using blebbistatin or the Rho kinase (ROCK) inhibitor compound Y27632 (Figs. 6A–6C and Supporting Information Movie 3). Conversely, induction of increased actomyosin contractility by expressing a constitutively active RhoA protein led to the formation of a large number of very elongated adhesion filaments (Fig. 6D).

New FA Linear Subunits Form at the Same Time as New Actin Radial Fibers

Next, we focused our attention on the mechanism of formation of new filaments in the same adhesion patch. We observed adhesion filaments and actin radial fibers at a high

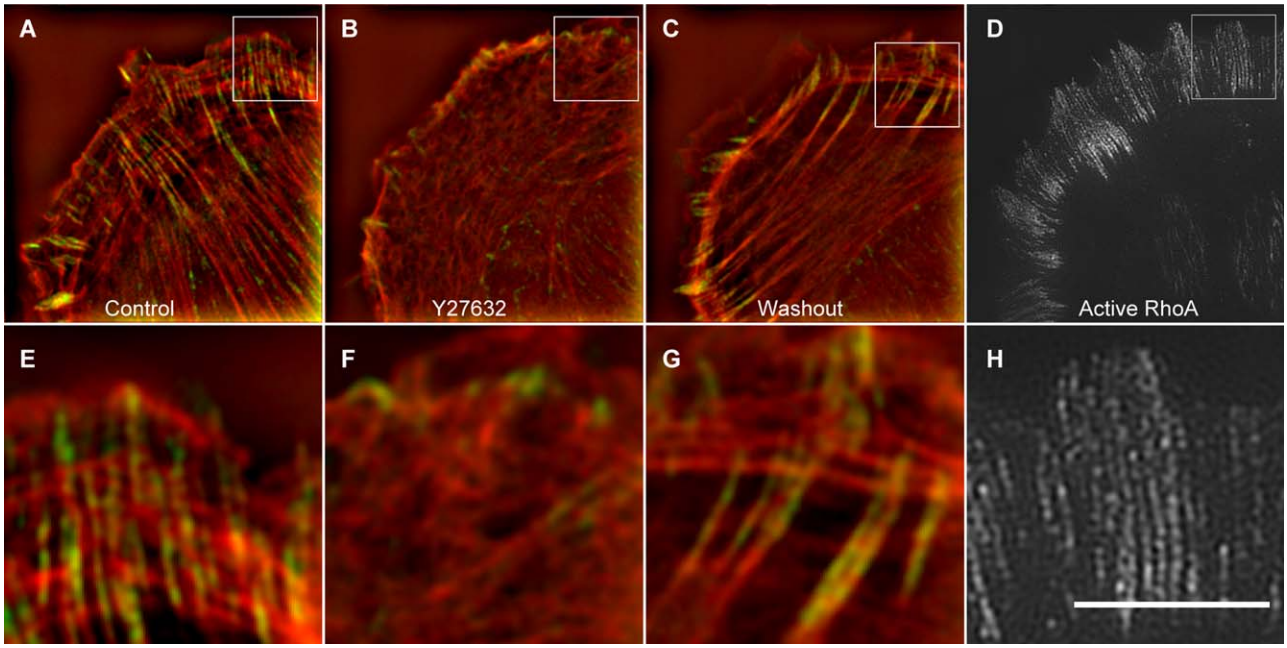

Fig. 6. Actomyosin contractility plays a role in focal adhesion subunit shape and dynamics. **A, B**: Cells were doubly transfected to express F-tractin–RFP (as a proxy for actin) and paxillin–eGFP (as a proxy for focal adhesions) and imaged using dual color SIM (A). The cells were treated with the Rock inhibitor Y27632, resulting in the disappearance of both actin cables and focal adhesions (imaged after 25 min, B). Washing out the rock inhibitor led to restoration of the actin cytoskeleton and linear focal adhesion subunits (imaged after 50 min, **C**). **D**: REF52 cells were transfected to express constitutively active RhoA, leading to an increase in the length of the subunits, while their width remained similar to that of wild-type REF52 cells (around 300 nm). E–H are magnified images of A–D. Scale bar is 5 μm. [Color figure can be viewed in the online issue, which is available at wileyonlinelibrary.com.]

resolution using dual color SIM in REF52 cells transfected with F-tractin RFP and paxillin–GFP. In contrast with what could be observed using conventional TIRF microscopy, dual color SIM revealed the formation and extension of FA linear subunits is an extremely rich, complex process. In particular, although the width of each adhesion filament remained constant, new linear subunits formed adjacent to existing linear subunits. As shown in Figures 7A and 7C, a group of linear subunits typically elongated and developed via successive appearance of parallel linear subunits. Importantly, all such filaments usually displayed relatively well-synchronized elongation and dynamics (Figs. 7A–7C and Supporting Information Movies 2 and 4). Moreover, each time a new adhesion linear subunit formed, we observed the formation of a new actin radial fiber (or the converse). In the example displayed in Figure 7, the number of subunits increased from 0 to 6 within typically 20 min, and the number of actin radial fibers increased accordingly. This demonstrates the existence of a tight relationship between the formation and morphology of FA linear subunits and actin radial fibers.

Discussion

Although TIRF microscopy has been instrumental in observing FA proteins, it provides limited information on the inner structure of these adhesion patches. SIM enables visualization of FAs at a high enough resolution to observe individual linear subunits, which are linked to separate actin cables and have a well-defined width and spacing. Additionally, it is also possible to observe the dynamics of FAs using SIM, which makes this technique a very powerful tool for the quantitative study of mechanosensing units in eukaryotic cells. We showed that FAs in REF52 cells are in fact composed of a stack of quasi-periodically-spaced linear subunits containing the major adhesion proteins (paxillin, zyxin, FAKs, VASP, integrin). This inner structure is normally not visible when imaging cells using conventional optical microscopes due to their low optical resolution. High-resolution structures of focal adhesions have been addressed in several previous studies, in which mainly fixed cells were observed by cryoelectron tomography (Patla etal., 2010), atomic force microscopy [Franz and Müller, 2005] and PALM [Kanchanawong et al., 2010; Shroff et al., 2007]. The interest of our approach with SIM–TIRFF is to reveal both the focal adhesion organization and their dynamics. Here, our observations add to previous reports by showing that the basic internal organization of FAs takes the form of quasi-parallel linear subunit with a well-defined width. Yet, the interior of such linear subunits is very likely not homogeneous, but rather also presents an ultrastructure as recently suggested by Shibata et al. [2012, 2013]. Indeed, Shroff et al. [2007] mentioned that the aggregating dots of FAs they observed in PALM follow a filament like

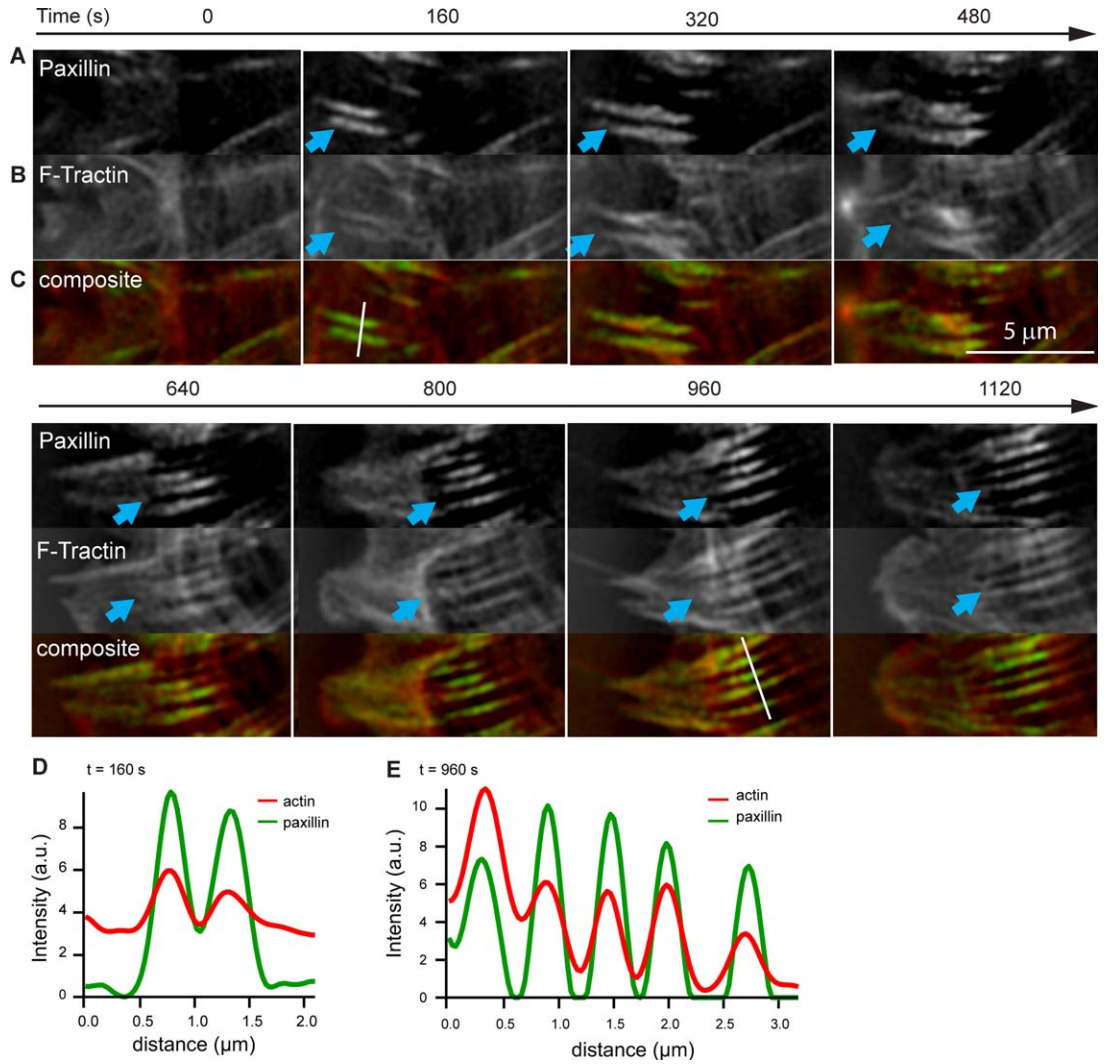

Fig. 7. Formation of focal adhesion linear filaments correlates with the formation of actin radial fibers. Cells were doubly transfected to express F-tractin–RFP (as a proxy for actin) and paxillin–eGFP (as a proxy for focal adhesions) and imaged using dual color SIM. **A–C**: Time-lapse images of paxillin (A), F-tractin (B), and the merged images (C) are shown as a function of time. The border of the cell is on the left, and the linear units elongate towards the center of the cell. The blue arrow shows a developing set of adhesion filaments for which the number of linear adhesion subunits increases from 0 to 6 in typically 20 min. Actin radial fibers appeared at the same rhythm, while transverse arc flow was faster than both the elongation rate for focal adhesion filaments and the appearance of new adjacent filaments (see Supporting Information Movie 4). **D–E**: Intensity profiles over a cross section of adhesion filaments for paxillin (green) and actin (red) at two different time points (160 and 960 s), showing that both proteins are structured as two aligned arrays of linear units. [Color figure can be viewed in the online issue, which is available at wileyonlinelibrary.com.]

organization. They are probably similar to FAs linear subunits we report in this work. In addition, we were able to study both the morphology and formation of these structures in conjunction with actomyosin contractility. We showed that the linear units have a well-defined width (300 ± 100 nm) but vary in length depending on actomyosin contractility. We also showed that each linear unit can elongate at a rate of about 0.1–0.8 μm/min with different phases during their life cycle (elongation, rest, and shortening). The origin of retrograde flow at the scale of adhesion plaques was previously attributed to actomyosin contractility. Indeed, we showed that the linear subunits shortened dramatically when the cells were treated with the ROCK inhibitor Y27632. Thus, the formation of FA linear units is dependent on actomyosin contractility. Increasing cell contractility by expressing constitutively active RhoA led to FAs with numerous linear units that had a long length, but comparable width to that of wild-type cells. Taken together, this suggests that the linear subunits are formed at the same time than the linked radial actin cable, and that their length is set by the actomyosin contractility of the cell. Further studies should focus on the biological processes that regulate the length of FA linear subunits. We found the presence of FA linear subunits in several cell types (REF52, Hela, HUVEC, and 3T3 MEF cells). However, we did not observe them in U2OS cells (Supporting Information Fig. 2). Interestingly,

U2OS cells show less FAs as well as less actin stress fibers compared to the other cell types. We do not know the mechanism that drives this difference, but it may be the result of different basal level of actomyosin contractility. This question will be addressed in our future studies.

FA plaques are often described as mechanosensor units [Bershadsky et al., 2003; Choquet et al., 1997; Geiger et al., 2009; Riveline et al., 2001], and are more developed (i.e., larger) on rigid substrates than soft substrates [Pelham and Wang, 1997; Prager-Khoutorsky et al., 2011]. Moreover, formation of FA plaques has been shown to be triggered by application of a local force [Riveline et al. 2001]. However, there is still no satisfying understanding of the mechanosensing ability of FA plaques. Similarly, the mechanism by which FA plaque formation is linked to actomyosin contractility remains elusive. In particular, it remains unclear to what extent their biophysical properties (shape and dynamics) are set locally by the mechanical properties of the substrate or, on the contrary, are regulated at the cellular scale via membrane tension or actin meshwork contractility. Importantly, it was reported that the area of FA plaques correlates with the pulling strength of the cell. In particular, using traction force microscopy, Balaban et al. determined that the FAs of REF52 cells exert a relatively constant force per unit area of 5.5 ± 2 nN μm^{-2}. This implies that large FA plaques can sustain larger forces than smaller FA plaques. Recently, this idea was challenged by measurement of forces exerted by cells on an array of micropillars: different forces were exerted by FAs of similar sizes [Trichet et al., 2012]. This was also discussed in a more general context by Gardel's lab: they showed using traction force microscopy that a correlation between FA morphology and traction forces was only observed during the first stages of adhesion maturation and growth [Stricker et al., 2011]. Here, we show that the area of a FA patch is not the relevant morphological parameter, rather its length and numbers of filament subunits. Indeed, actin cables pulling on nascent FAs extend the FA subunit, although the creation of new filaments together with the formation of new actin radial fibers. Force measurements based on arrays of micropillars naturally constrain the area on which linear FA subunits can develop and, as such, strongly limit the length of the FA subunits. With this in mind, it appears that the stress that a FA plaque can sustain is likely to be different on a micropillar array than on a 2D surface. Therefore, the identification of linear unit structures should be taken into account during experimental design and also to improve modeling of the growth and mechanosensing ability of FAs.

Materials and Methods

Cell Culture, Plasmids, and Transfection

The plasmid used to express paxillin–tdEos, paxillin–eGFP, and paxillin–mApple were provided by Dr. Pakorn Kanchanawong (Mechanobiology Institute, NUS, Singapore). FTractin–RFP was the gift from Dr. Michael J. Schell (Uniformed Services University, Bethesda, MD). Other plasmids were previously used in the laboratory of Weizmann Institute of Science, Rehovot, Israel. REF52 cells and stably expressing paxillin–YFP REF52 cells were previously used in the laboratory of Weizmann Institute of Science. Cells were transfected via electroporation using the Neon transfection system (MPK1096; Invitrogen) following the standard protocol. All cells were cultured in Dulbecco's modified Eagle's medium (DMEM; 11965092, Invitrogen) containing 10% fetal bovine serum (FBS; 10082147, Invitrogen) and 1% penicillin–streptomycin (15070063, Invitrogen) at 37°C in a 5% CO_2 humidified incubator. Typically, 10^4 cells were plated on a 25 mm round coverslip, which had been precoated with fibronectin (11080938001, Roche), and incubated for 20–30 min. Then floating cells were gently washed away, the coverslips were incubated for 3 h unless stated otherwise, the coverslips were mounted onto the observation chamber (CM-B25-1 Chamlide CMB chamber) and the media was changed to fresh Leibovitz's medium with 10% FBS and 1% penicillin–streptomycin before microscopy imaging.

Phalloidin Staining

Phalloidin 594 was obtained from Invitrogen (A12381, Invitrogen). For staining, cells were fixed in warm 4% paraformaldehyde (PFA; P-6148, Sigma-Aldrich) for 20 min at 37°C, washed in PBS (BUF-2040 1st Base), permeabilized with 0.1% Triton X-100 (Sigma-Aldrich) for 7 min at room temperature, blocked in 3% bovine albumin serum (BSA; A7906, Sigma-Aldrich) for 1 h, and incubated with phalloidin 594 for 20 min.

Micropatterning and Fibronectin Coating

Fibronectin-coated micropatterns were produced on glass coverslips by deep UV patterning as described in Azioune et al. [2010]. Briefly, clean glass coverslips (No. 1.5H 25 mm round coverslip; 017650, Marienfeld) were coated with 50 µl of 0.15 mg/ml PLL(20)–g(3.5)–PEG(2) (SuSoS) in 10 mM HEPES at pH 7.4 for 2 h. PLL(20)–g(3.5)–PEG(2) coated glass coverslip was illuminated under an 185 nm UV lamp (UVO cleaner, Jelight) through a quartz photomask (produced locally at MBI) for 8 min. Then the UV activated glass coverslips were incubated with 50 µl of 25 µg/ml fibronectin (11080938001, Roche) in 100 mM $NaHCO_3$ at pH 8.6 for 1 h. For direct homogeneous coating, glass coverslips are directly incubated with 25 µg/ml fibronectin for 1 h at room temperature.

Microscopes and Live Cell Imaging

Fixed cells and live cells were imaged by structured illumination microscopy (N-SIM; Nikon) [Trichet et al., 2012], total internal reflection fluorescence microscopy (TIRF;

Nikon Ti-E) or stochastic optical reconstruction microscopy (STORM; Nikon Ti-E). The SIM images were taken in SIM–TIRF mode (based on TIRF, we used this when imaging a single FA protein) or dual color SIM mode (based on full illumination, we used this when imaging two fluorescent proteins simultaneously) using an 100× oil (NA 1.49) objective with autofocus maintained by the Nikon Perfect Focus system. The samples were mounted in a homemade cell culture chamber and maintained at 37°C. The same EM CCD camera (DU897, Andor Technology) and 100× oil (NA 1.49) objective were used for both TIRF and STORM imaging. For the STORM system, 10,000–50,000 images were acquired at 30 ms per frame and then reconstructed into a single frame using Nikon software.

Imaging Analysis

We computed the 2D spatial autocorrelation to calculate the average width and spatial period of FA filaments. The code for autocorrelation analysis was written in Matlab and automated statistics analysis was performed using the technical graphing and data analysis software Igor Pro (WaveMetrics, Lake Oswego, OR). For the autocorrelation analysis, we first extracted a small region of interest (ROI) which contained several closely aligned FA linear subunits, and then computed its 2D autocorrelation. This gives us a 2D autocorrelation image from which we can extract the distance between the origin and the first minima in all possible orientations. We then extracted the orientation that gives the closest minima which corresponds to the direction perpendicular to the array of linear subunits. The width is measured as twice the distance between the origin and the first minima. The spacing is defined as the distance between the origin and the first maxima. Lengths and widths of filaments were also manually extracted based on the intensity profile of the image; this data was used to compute the velocity of extension and retraction of the linear filaments. For image analysis, we used ImageJ (http://www.rsb.info.nih.gov/ij). Single filaments could be easily followed by processing the image as follows: the raw image was averaged every five frames, then we used the "unsharp mask filter", "auto thresholding" and the "magic wand" tool to obtain a mask representing the morphology of the linear subunits.

Acknowledgments

The authors would like to thank our respective team members for critical reading of this manuscript, as well as Jean-Marc Di Meglio (University Paris Diderot, France) and Benoit Sorre (CNRS, France) for insightful discussions. A.D. Bershadsky holds the Joseph Moss Professorial Chair in Biomedical Research at the Weizmann Institute and is a visiting professor at the National University of Singapore, and acknowledges support from Israel Science Foundation (grant No. 956/10). This work was supported by the Mechanobiology Institute (MBI), the Laboratoire International Associé Cell Adhesion France-Singapour (CAFS), the Agence Nationale de la Recherche (ICEBERG-ANR-10-BINF-06-01) and the Who am I? Laboratory of Excellence (ANR-11-LABX-0071 and ANR-11-IDEX-0005-01).

Author Contributions

Author Contributions: SH performed all experiments and numerical analysis; SH, AK and PH analyzed the data; SH, YH, RZB, AK, AB, PH contributed experimental design, analysis and important ideas; AB, AK, PH and RZB wrote the manuscript.

References

Alexandrova AY, et al. 2008. Comparative dynamics of retrograde actin flow and focal adhesions: formation of nascent adhesions triggers transition from fast to slow flow. PloS One 3:e3234.

Azioune A, Carpi N, Tseng Q, Théry M, Piel M. 2010. Protein micropatterns: a direct printing protocol using deep UVs. Methods Cell Biol 97:133–146.

Bershadsky AD, Balaban NQ, Geiger B. 2003. Adhesion-dependent cell mechanosensitivity. Ann Rev Cell Devlop Biol 19:677–695.

Choquet D, Felsenfeld DP, Sheetz MP. 1997. Extracellular matrix rigidity causes strengthening of integrin-cytoskeleton linkages. Cell 88:39–48.

Discher DE, Janmey P, Wang Y-L. 2005. Tissue cells feel and respond to the stiffness of their substrate. Science (New York, NY) 310:1139–1143.

Eyckmans J, Boudou T, Yu X, Chen CS. 2011. A hitchhiker's guide to mechanobiology. Dev Cell 21:35–47.

Franz CM, Müller DJ. 2005. Analyzing focal adhesion structure by atomic force microscopy. J Cell Sci 118:5315–5323.

Gardel ML, et al. 2008. Traction stress in focal adhesions correlates biphasically with actin retrograde flow speed. J Cell Biol 183:999–1005.

Geiger B, Spatz JP, Bershadsky AD. 2009. Environmental sensing through focal adhesions. Nat Rev Mol Cell Biol 10:21–33.

Guo W, Wang Y. 2007. Retrograde fluxes of focal adhesion proteins in response to cell migration and mechanical signals. Mol Biol Cell 18:4519–4527.

Guo C-L, Harris NC, Wijeratne SS, Frey EW, Kiang C-H. 2013. Multiscale mechanobiology: mechanics at the molecular, cellular, and tissue levels. Cell Biosci 3:25.

Gustafsson MG. 2000. Surpassing the lateral resolution limit by a factor of two using structured illumination microscopy. J Microsc 198:82–87.

Hu K, Ji L, Applegate KT, Danuser G, Waterman-Storer CM. 2007. Differential transmission of actin motion within focal adhesions. Science (New York, NY) 315:111–115.

Kanchanawong P, et al. 2010. Nanoscale architecture of integrin-based cell adhesions. Nature 468:580–584.

Patla I, et al. 2010. Dissecting the molecular architecture of integrin adhesion sites by cryo-electron tomography. Nature Cell Biology 12:909–15.

Pelham RJ, Wang Y. 1997. Cell locomotion and focal adhesions are regulated by substrate flexibility. Proc Natl Acad Sci USA 94: 13661–13665.

Prager-Khoutorsky M, et al. 2011. Fibroblast polarization is a matrix-rigidity-dependent process controlled by focal adhesion mechanosensing. Nat Cell Biol 13:1457–1465.

Riveline D, et al. 2001. Focal contacts as mechanosensors: externally applied local mechanical force induces growth of focal contacts by an mDia1-dependent and ROCK-independent mechanism. J Cell Biol 153:1175–1185.

Seong J, Wang N, Wang Y. 2013. Mechanotransduction at focal adhesions: from physiology to cancer development. J Cell Mol Med 17:597–604.

Shroff H, et al. 2007. Dual-color superresolution imaging of genetically expressed probes within individual adhesion complexes. Proc Natl Acad Sci USA 104:20308–20313.

Shibata ACE, et al. 2012. Archipelago architecture of the focal adhesion: membrane molecules freely enter and exit from the focal adhesion zone. Cytoskeleton 69:380–392.

Shibata ACE, et al. 2013. rac1 recruitment to the archipelago structure of the focal adhesion through the fluid membrane as revealed by single-molecule analysis. Cytoskeleton 70:161–177.

Smilenov LB. 1999. Focal adhesion motility revealed in stationary fibroblasts. Science 286:1172–1174.

Stricker J, Aratyn-Schaus Y, Oakes PW, Gardel ML. 2011. Spatiotemporal constraints on the force-dependent growth of focal adhesions. Biophys J 100:2883–2893.

Vicente-Manzanares M, Zareno J, Whitmore L, Choi CK, Horwitz AF. 2007. Regulation of protrusion, adhesion dynamics, and polarity by myosins IIA and IIB in migrating cells. J Cell Biol 176:573–580.

Vicente-Manzanares M, Ma X, Adelstein RS, Horwitz AR. 2009. Non-muscle myosin II takes centre stage in cell adhesion and migration. Nat Rev Mol Cell Biol 10:778–790.

Vogel V. 2006. Mechanotransduction involving multimodular proteins: converting force into biochemical signals. Ann Rev Biophys Biomol Struct 35:459–488.

Vogel V, Sheetz M. 2006. Local force and geometry sensing regulate cell functions. Nat Rev Mol Cell Biol 7:265–275.

Winograd-Katz SE, Fässler R, Geiger B, Legate KR. 2014. The integrin adhesome: from genes and proteins to human disease. Nat Rev Mol Cell Biol 15:273–288.

Wolfenson H, Henis YI, Geiger B, Bershadsky AD. 2009. Cell motility and the cytoskeleton. 66:1017–1029.

Trichet L, et al. 2012. Evidence of a large-scale mechanosensing mechanism for cellular adaptation to substrate stiffness. PNAS 109: 6933–6938. 3

Zaidel-Bar R, Itzkovitz S, Ma'ayan A, Iyengar R, Geiger B. 2007. Functional atlas of the integrin adhesome. Nat Cell Biol 9:858–867.